Aquatic Toxicology 226 (2020) 105558

Contents lists available at ScienceDirect

Aquatic Toxicology

journal homepage: www.elsevier.com/locate/aqtox

Expression and localization of the aryl hydrocarbon receptors and cytochrome P450 1A during early development of Atlantic cod (*Gadus morhua*)

Libe Aranguren-Abadía[a], Carey E. Donald[b], Mariann Eilertsen[a], Naouel Gharbi[c], Valentina Tronci[c], Elin Sørhus[b], Philipp Mayer[d], Tom Ole Nilsen[a], Sonnich Meier[b], Anders Goksøyr[a,b], Odd André Karlsen[a,*]

[a] Department of Biological Sciences, University of Bergen, Bergen, Norway
[b] Institute of Marine Research, Bergen, Norway
[c] NORCE Norwegian Research Centre AS, Uni Research Environment, Bergen, Norway
[d] Department of Environmental Engineering, Technical University of Denmark, Lyngby, Denmark

ARTICLE INFO

Keywords:
Atlantic cod
Early development
Aryl hydrocarbon receptor (Ahr)
Cytochrome P450 1A (Cyp1a)
In situ hybridization

ABSTRACT

The aryl hydrocarbon receptor (Ahr) is a ligand-activated transcription factor that mediates the toxicity of dioxins and dioxin-like compounds (DLCs) in vertebrates. Two clades of the Ahr family exist in teleosts (Ahr1 and Ahr2), and it has been demonstrated that Ahr2 is the main protein involved in mediating the toxicity of dioxins and DLCs in most teleost species. Recently, we characterized the Atlantic cod (*Gadus morhua*) Ahr1a and Ahr2a receptors. To further explore a possible subfunction partitioning of Ahr1a and Ahr2a in Atlantic cod we have mapped the expression and localization of *ahr1a* and *ahr2a* in early developmental stages. Atlantic cod embryos were continuously exposed in a passive-dosing exposure system to the Ahr agonist, benzo[*a*]pyrene (B[a]P), from five days post fertilization (dpf) until three days post hatching (dph). Expression of *ahr1a*, *ahr2a*, and the Ahr-target genes, *cyp1a* and *ahrrb,* was assessed in embryos (8 dpf and 10 dpf) and larvae (3 dph) with quantitative real-time PCR analyses (qPCR), while *in situ* hybridization was used to assess the localization of expression of *ahr1a*, *ahr2a* and *cyp1a*. Quantitative measurements showed an increased *cyp1a* expression in B[a]P-exposed samples at all sampling points, and for *ahr2a* at 10 dpf, confirming the activation of the Ahr-signalling pathway. Furthermore, B[a]P strongly induced *ahr2a* and *cyp1a* expression in the cardiovascular system and skin, respectively, of embryos and larvae. Induced expression of both *ahr2a* and *cyp1a* was also revealed in the liver of B[a]P-exposed larvae. Our results suggest that Ahr2a is the major subtype involved in mediating responses to B[a]P in early developmental stages of Atlantic cod, which involves transcriptional regulation of biotransformation genes, such as *cyp1a*. The focused expression of *ahr1a* in the eye of embryos and larvae, and the presence of *ahr2a* transcripts in the jaws and fin nodes, further indicate evolved specialized roles of the two Ahrs in ontogenesis.

1. Introduction

The aryl hydrocarbon receptor (Ahr) is a ligand activated transcription factor that has existed for more than 600 millon years of animal evolution, and it is broadly distributed in multiple phyla (Hahn et al., 2017). Ahr is a member of the basic helix-loop-helix/Per-Arnt-Sim family and has been extensively studied in toxicology because of its role in mediating responses to many xenobiotic compounds in vertebrates (Nebert, 2017; Okey, 2007). As a result of a tandem duplication of Ahr prior to the divergence of the cartilaginous and bony fish linegaes, two Ahr clades exist: Ahr1 and Ahr2 (Hahn et al., 2017; Karchner et al., 2005). In addition, due to the teleost-specific whole genome duplication, fishes can have multiple paralogous *ahr* genes (Glasauer and Neuhauss, 2014).

A diverse group of environmental pollutants, as well as endogenous compounds, are known to bind and activate Ahr, including dioxins, dioxin-like polychlorinated biphenyls, and polycyclic aromatic hydrocarbons (PAHs) (Denison and Nagy, 2003). The toxicity of PAHs and other crude oil components has been widely studied in fishes, especially during embryonic development and early life stages (Anderson et al.,

* Corresponding author at: Department of Biological Sciences, University of Bergen, P.O. box 7803, N-5020, Bergen, Norway.
E-mail address: Odd.Karlsen@uib.no (O.A. Karlsen).

https://doi.org/10.1016/j.aquatox.2020.105558
Received 26 February 2020; Received in revised form 25 June 2020; Accepted 1 July 2020
Available online 03 July 2020

1974; Barron et al., 2004; Goksøyr et al., 1994; Hylland et al., 2008; Sørhus et al., 2015). Ahr2 is the main protein involved in mediating xenobiotic responses to such compounds in most fish species (Tanguay et al., 1999; Walker et al., 1991; Zanette et al., 2009), as demonstrated in loss-of-function studies using morpholino-modified antisense oligonucleotides or genome editing (Clark et al., 2010; Garcia et al., 2018; Goodale et al., 2012; Jönsson et al., 2007, 2009; Prasch et al., 2003; Sugden et al., 2017).

Unliganded Ahr is located in the cytoplasm in a protein complex with two HSP90 proteins, a co-chaperon protein p23, and Ahr-interacting protein (AIP) (Carver and Bradfield, 1997; Denison et al., 2011; Kazlauskas et al., 1999; Perdew, 1988). The recognition and binding to an agonist promote the conformational activation of Ahr and subsequent translocation into the nucleus where Ahr heterodimerizes with the aryl hydrocarbon receptor nuclear translocator (Arnt). This heterodimer binds to xenobiotic response elements (XRE) upstream of Ahr target genes and modulate the transcription of different enzymes involved in the biotransformation of xenobiotics, including cytochrome P450 1A (Cyp1a) (Denison et al., 2011; Pollenz et al., 1993; Soshilov and Denison, 2008; Swanson, 2002; Whitlock, 1999). Another Ahr target gene is the aryl hydrocarbon receptor repressor (Ahrr), which has a role in regulating Ahr transcriptional activity. Different mechanisms of Ahrr-mediated repression of the activity of Ahr have been postulated, including a crystallography study that showed the formation of an Ahrr-Arnt heterodimer (Mimura et al., 1999; Sakurai et al., 2017).

During the last decades different studies have highlighted the role of Ahr in signalling pathways and physiological systems other than the response to xenobiotic compounds, including the cardiovascular, reproductive and immune system in vertebrates (Esser and Rannug, 2015; Mulero-Navarro and Fernandez-Salguero, 2016; Nebert, 2017). It has been suggested that the original function of Ahr was to regulate the development of neural systems and sensory structures, and that these ancestral functions are still present in modern living invertebrates (Hahn et al., 2017). Hahn et al. suggested a specialization of the different *ahr* paralogs through subfunction partitioning in some non-mammalian vertebrates (Hahn et al., 2017). Some of the partitioning mechanisms described include tissue-specific expression patterns, as well as ligand- and target gene specificity. An example is the zebrafish, whose three Ahrs are thought to have evolved different functional roles. While the Ahr2 of zebrafish (zfAhr2) is involved in mediating toxic responses to dioxin-like compounds and PAHs, zfAhr1b is suggested to have a role in embryonic development (Karchner et al., 2005). zfAhr1a, on the other hand, is not activated by any classical Ahr agonists, but may still be involved in the regulation of physiological responses by being activated by a variety of non-halogenated compounds (Chlebowski et al., 2017; Goodale et al., 2012; Incardona et al., 2006; Knecht et al., 2013). A role of zfAhr2 in the development of the nervous and sensory system has also been demonstrated (Garcia et al., 2018; Goodale et al., 2012; Souder and Gorelick, 2019).

Atlantic cod (*Gadus morhua*) has for many years been used as an indicator species in marine pollution monitoring programs and field studies (Beyer et al., 1996; Dale et al., 2019; Goksøyr et al., 1994; Hylland et al., 2008; OSPAR, 2010; Sundt et al., 2012). However, in order to obtain a better understanding of how cod mediates responses to pollutants, we recently functionally described the Ahr1a and Ahr2a receptors for the first time (Aranguren-Abadía et al., 2020). These paralogous genes differed in their tissue-specific expression in juvenile cod, as well as possessing different ligand binding affinities and transactivation activities, which may indicate a subfunctional partitioning of the Ahr receptors in this species.

The aim of the present study was to further explore a possible subfunction partitioning of Ahr1a and Ahr2a in Atlantic cod by mapping the expression and localization of *ahr1a*, *ahr2a* and *cyp1a* in early developmental stages. Activation of the Ahr-signalling pathway was confirmed by measuring expression of *cyp1a* in B[a]P-exposed samples. Our results suggest that Ahr2a is the major subtype involved in mediating responses to B[a]P in early developmental stages of Atlantic cod. Furthermore, expression of *ahr2a* in developing jaws and fin nodes of larvae, and the persistent presence of *ahr1a* transcripts in the eye of both cod embryo and larvae indicates a physiological role of these genes in the ontogenesis of these organs.

2. Material and methods

2.1. Passive-dosing exposure experiment

2.1.1. Cleaning and loading of silicone rods

Water exposure of highly hydrophobic compounds like B[a]P is challenging due to the very low water solubility and high absorption to surfaces in the exposure tanks. Passive dosing was chosen to establish and maintain freely dissolved concentrations of B[a]P at the solubility limit, while avoiding co-solvent addition (Smith et al., 2010). Translucent 1-mm silicone rods (Altec Extrusions, Victoria, UK) were cut to 1 m lengths and precleaned by soaking in methanol and ultrapure water washes. All chemicals used were GC Suprasolv® analytical grade and supplied by Merck (Darmstadt, Germany). The rods were then loaded into saturated B[a]P methanol solutions for two days, whereas control-rods were immersed in methanol (> 99 % purity, Sigma-Aldrich, St. Louis, Missouri, United States) (Smith et al., 2010). After the loading, excess methanol was removed by three successive soaks in ultrapure water for 2–24 hours. One corresponding rod was allowed to equilibrate with 80 mL of autoclaved seawater in each glass beaker for two days before the start of the exposures. All glassware was heated to 400 °C overnight before use.

2.1.2. Exposure of Atlantic cod eggs

Eggs and sperm were stripped from brood stocks of Atlantic cod (*Gadus morhua*), and the eggs were fertilized *in vitro* at the Institute of Marine Research (IMR), Austevoll Research station. Fertilized eggs were transferred to indoor egg incubators, and maintained at 7 ± 1 °C until transported to IMR's facilities in Bergen to begin the exposure studies at 5 days post fertilization (dpf), when the cardiac cone of cod embryos is visible. About 200 eggs were placed randomly in the prepared exposure beakers of either B[a]P or seawater (control group). There were four replicate beakers for each treatment and an additional beaker without eggs (water control) for each group. Exposure to B[a]P started at 5 dpf and lasted until 3 days post hatching (dph). The experiment took place in a cold room at 8 °C, and the temperature in the water and in the room was monitored during the experiment. Dead eggs were removed during daily inspections from all the beakers to minimize bacterial contamination. Samples of several embryos and larvae were collected at 8 dpf, 10 dpf and 3 dph for gene expression and *in situ* hybridization analyses.

2.1.3. Water chemistry and body burden analyses

Water samples (1.0 mL) were taken at 5 dpf, 8 dpf, 11 dpf and 3 dph and liquid-liquid extracted with two 1-mL volumes of dichloromethane (SupraSolv®, Merck, Darmstadt, Germany). Extracts were dried with Na_2SO_4, and exchanged into 200 µL isopropanol (EMSURE®, Merck, Darmstadt, Germany). Twenty eggs were collected from each replicate jar at 8 dpf. These body burden samples were homogenized and extracted twice as in (Sørensen et al., 2019), with 50 % dichloromethane in *n*-hexane (SupraSolv®, Merck, Darmstadt, Germany) and subsequent clean-up with solid-phase extraction (Chromabond® silica, 3 mL, glass, Macherey-Nagel, Dueren, Germany). Water and body burden analyses for B[a]P and internal standard were performed on an Agilent 6890 gas chromatograph coupled to a 7010 triple quadrupole mass spectrometer as described in (Sørensen et al., 2016). Statistical differences in body burden concentration between control and B[a]P-exposed groups were analyzed using a Welch's *t*-test in R v1.2.1335 software (Crawley, 2012).

2.2. Quantitative polymerase chain reaction (qPCR) analyses

Total RNA was isolated from ten pooled samples of embryos or larvae from each beaker (n = 4) at 8 dpf, 10 dpf and 3 dph using the TRI Reagent® protocol (Sigma-Aldrich, St. Louis, Missouri, United States) as outlined by Chomczynski, 1993. 500 ng of total RNA was reverse transcribed to cDNA using the iScriptTM cDNA Synthesis Kit (Bio-Rad, California, USA) following the provider's protocol. Quantitative real-time polymerase chain reaction analyses (qPCR) were performed using SYBR Green Master I (Roche Diagnostics, Mannheim, Germany) and a CFX96 Touch Real-Time PCR Detection System (Bio-Rad, California, USA) as described in (Aranguren-Abadía et al., 2020). Elongation factor 1 alpha (*ef1a*) and ubiquitin (*ubi*) were used as reference genes (Table S1) for normalization of gene expression across samples, and the geNorm software (Vandesompele et al., 2002) was used to calculate the normalization factor based on the geometric mean. The geNorm stability index M for the reference genes was 0.97. Relative induction of *ahr1a*, *ahr2a*, *cyp1a* and *ahrrb* genes (Table S1) between control and B[a]P-exposed groups was analyzed at the different sampling points using a Welch *t*-test on log transformed data in R v1.2.1335 software.

2.3. In situ hybridization (ISH)

2.3.1. Tissue preparation for in situ hybridization

Cod embryos at 8 and 10 dpf and larvae at 3 dph were fixed in 4% paraformaldehyde buffered in 1x phosphate-buffered saline (PBS) solution (pH 7.4) for 48 h at 4 °C for whole mount *in situ* hybridization. Whole mount embryos and larvae were briefly washed in 1x PBS, dehydrated in methanol, and stored in 100 % methanol at −20 °C until use. Larvae for tissue sections *in situ* hybridization were fixed in 4% paraformaldehyde-buffered in 1x PBS for 48 h at 4 °C, incubated in a solution of 25 % sucrose, 25 % Tissue Tek (Sakura Finetek, California, United States) and 50 % 1x PBS overnight at 4 °C before they were oriented and embedded in Tissue Tek and kept at −80 °C.

2.3.2. Molecular cloning

Cloning of *ahr1a* and *ahr2a* genes has been previously described in (Aranguren-Abadía et al., 2020). A partial sequence of *cyp1a* was amplified as a single fragment from cDNA prepared from juvenile cod heart using Taq DNA polymerase (Invitrogen, California, USA) and specific primers (Table S1). The *cyp1a* fragment was inserted into a pCR™4Blunt-TOPO® vector (Thermo Fisher, Massachusetts, USA), and DNA sequencing was performed at the University of Bergen Sequencing Facility.

2.3.3. Synthesis of ahr1a, ahr2a and cyp1a RNA probes

Preparation of digoxigenin (DIG)-labelled riboprobes for *ahr1a, ahr2a* and *cyp1a* were done following the manufacturer's instructions (Roche Diagnostics, Mannheim, Germany). In the synthesis of the riboprobes, PCR products was used as template for the reactions as described in (Thisse and Thisse, 2008) (Table 1) and the synthesized probes were precipitated by LiCl and EtOH together with tRNA (Roche Diagnostics, Mannheim, Germany). Further, *ahr1a* and *ahr2a* probes were designed in the less conserved coding sequence region in order to avoid cross-hybridization of probes between the paralogous genes.

2.3.4. Whole mount in situ hybridization

Whole mount *in situ* hybridization of embryos and larvae (n = 3 per gene and sampling point) were performed as described in (Valen et al., 2014). Briefly, embryos and larvae were rehydrated in methanol (75 − 25%) followed by dechorination of embryos. Pigmentation of embryos and larvae was removed by bleaching in 3% Hydrogen peroxide (H_2O_2)/0.5 % Potassium hydroxide (KOH) (Sigma-Aldrich, St. Louis, Missouri, United States). Prior to hybridization, the embryos and larvae were treated with Proteinase K (Promega, Wisconsin, United States). After hybridization, the tissue was thoroughly washed and treated with RNase A (Sigma-Aldrich, St. Louis, Missouri, United States) to remove unhybridized probe. Before applying the antibody (anti-DIG conjugated with alkaline phosphatase, Fab fragments (1:2000) (Cat. No 11093274910, Roche Diagnostics, Mannheim, Germany, RRID: AB_514497)) the embryos and larvae were incubated in 2% blocking solution (Roche Diagnostics, Mannheim, Germany) in 2x SSC with 0.05 % Triton X-100 (Sigma-Aldrich, St. Louis, Missouri, United States). The DIG-labelled probes were visualized by 4-nitro blue tetrazolium chloride (NBT) and 5-bromo-4-chloro-3-indolyl-phosphate system (BCIP) (Roche Diagnostics, Mannheim, Germany) and sense probes were used as a control for nonspecific DIG-probe labelling (data not shown).

2.3.5. Tissue sections in situ hybridization

In situ hybridization for *arh1a*, *arh2a* and *cyp1a* transcripts (sense and antisense) was performed on serial sections for n = 6 larvae per gene as described in (Ebbesson et al., 2011). By using a Cryostat (Leica CM 3050, Leica Microsystems, Wetzlar, Germany), 12 µm transversal sections were performed for each larvae and deposited into Superfrost Ultra Plus slides (Menzel-Gläser, Braunschweig, Germany). Proteinase K (Sigma-Aldrich, St. Louis, Missouri, United States) treatment was applied for 3.5 min and tissue sections were left 1 h at room temperature for drying prior to hybridization. Sections were treated with RNase (Roche Diagnostics, Mannheim, Germany) prior to incubation in antibody solution (1x maleate buffer + 1% block solution + 0,3% Triton X-100) with anti-digoxigenin alkaline phosphatase FAB-fragment (1:2000, (Roche Diagnostics, Mannheim, Germany)). Chromogen substrate (NBT/BCIP) (Roche Diagnostics, Mannheim, Germany) was applied for visualization of DIG-labelled probes and then mounted in 70 % glycerol for microscopy.

2.4. Imaging, craniofacial and cardiac analyses

Leica DMLB and M420 microscopes (Leica Microsystems, Wetzlar, Germany) with the camera Infinity 3 (Teledyne Lumenera, Ontario, Canada) and Image-Pro Premier 9.3 (Media Cybernetics, Rockville, Maryland, United States) were used for imaging of *in situ* hybridization samples. Adobe Photoshop CS5 (San Jose, California, United States) was used to adjust exposure, brightness and contrast in the pictures.

Larvae pictures and videos during the B[a]P-exposure were taken with an Olympus SZX-10 Stereo microscope equipped with a 1.2 Mp resolution video camera (Unibrain Fire-I 785c) controlled by BTV Pro 5.4.1 software (www.bensoftware.com). Larvae were immobilized in 3% methylcellulose and kept at 8 °C using a temperature controlled stage (Brook Industries, Illinois, United States). Length of mandible, ethmoid plate, area of edema and the ventricular and atrial diastolic (D)

Table 1
Overview of oligosequences used for probe synthesis. Promoter T3 and T7 sequences are marked in bold font.

Gene	Forward primer (5′-3′) with T3 promoter	Reverse primer (5′-3′) with T7 promoter	Probe size (bp)
ahr1a	**TAATACGACTCACTATAGGG**GCTGAGATGCTGCTGCATCTGCT	**CATTAACCCTCACTAAAGGGAA**CAGTCCAACCACCCCATTCCTGGATT	777
ahr2a	**TAATACGACTCACTATAGGG**CATCTGGTTGGAGAGCATCTGGTTGGA	**CATTAACCCTCACTAAAGGGAA**TGGACCAGGTGTTCATGGAGAGC	1026
cyp1a	**TAATACGACTCACTATAGGG**TTCTGGATGTTGGAGTTCTC	**CATTAACCCTCACTAAAGGGAA**TCTACATGCTCATGAAGTTCC	841
cyp1a	**TAATACGACTCACTATAGGG**TTCTGGATGTTGGAGTTCTC	**CATTAACCCTCACTAAAGGGAA**TCTACATGCTCATGAAGTTCC	841

and systolic diameter (S) used to estimate the fractional shortening (FS = (D–S)/D) were measured using Image J (Image J 1.52 t, National Institute of Health, Bethesda, Maryland, USA) with the object J plugin as described in (Sørhus et al., 2016). Differences in the length of jaw and ethmoid plate, edema area and FS between groups were assessed using one-way ANOVA and Tukey's multiple comparisons tests in R v1.2.1335 software.

3. Results

3.1. Water chemistry and body burden analyses

Atlantic cod eggs were kept in normal seawater or seawater with B[a]P-infused silicone rods from 5 dpf until 3 dph. The concentration of B[a]P in water was measured at four time points, and body burden of B[a]P was measured after 3 days of exposure (8 dpf). Measured B[a]P concentration in water across all analyzed samples ranged between 0.3 and 37 μg/L with an average of 7.6 μg/L in seawater at 7 °C (Fig. S1A).

The average body burden level in the B[a]P-exposed embryos was 14 ± 5 pg/embryo (range: 8–20); by wet weight, average body burden was 6.5 μg/kg wet weight (range: 3.7–9.2, Fig. S1B). Body burden in the B[a]P-exposed group was significantly greater ($p = 0.01$) than background levels present in the control group (0.36 μg/kg, Figure S1B). Although body burden samples were only collected at 8 dpf, B[a]P is presumed to have been absorbed throughout the duration of the experiment.

3.2. Expression of ahr1a, ahr2a, cyp1a and ahrrb in eggs and larvae

Samples of embryos and larvae were collected at 8 dpf, 10 dpf and 3 dph, and the expression of *ahr1a*, *ahr2a*, *cyp1a* and *ahrrb* genes was assessed with qPCR analyses (Fig. 1). The expression of *ahr1a* did not change notably between the control and B[a]P-exposed groups at the different sampling points, but expression of *ahr2a* increased slightly at 10 dpf ($p = 0.05$) (Fig. 1A, B). *cyp1a*-expression was induced in B[a]P-exposed samples at 8 dpf ($p = 0.01$), 10 dpf ($p = 0.001$) and 3 dph ($p = 0.00006$), reaching close to a 40-fold average induction in transcript levels at 10 dpf and 3 dph compared to the normal seawater control samples (Fig. 1C). Expression of *ahrrb* did not change between the control and B[a]P-exposed groups at the different sampling points (Fig. 1D).

3.3. Whole mount in situ hybridization of Atlantic cod embryo and larvae

The specific localization of *ahr1a*, *ahr2a*, and *cyp1a* expression was assessed in cod embryo and larvae using *in situ* hybridisation. At 8 dpf, the expression of *ahr1a* was evident in the eye of both controls and B[a]P-exposed embryos (Fig. 2A, B) (Fig. 2C, D). In contrast, differences in the *ahr2a* expression pattern was already detectable at this developmental stage (Fig. 2E, F), and *ahr2a* was only visible in the cardiovascular system of embryos exposed to B[a]P (Fig. 2G, H). An early effect of B[a]P-exposure on *cyp1a* expression was also visible, where its presence was detectable in the skin and vasculature of treated embryos (Fig. 2I, J). Expression of *cyp1a* was also localized in the heart and in the area where the liver develops in both control (Fig. 2L, M) and B[a]P-exposed embryos (Fig. 2O, P). There was not any visible expression of *cyp1a* in the eye of embryos from neither groups (Fig. 2K, N), as the staining present on the eye lens in B[a]P-exposed embryos corresponds to skin tissue (Fig. 2N).

At 10 dpf, *ahr1a* transcripts were present in the eye ganglion cell layer of embryos independent of their exposure regime (Fig. 3A, B, C, D). Notably, at this stage the expression of *ahr2a* was strongly visible in the cardiovascular system of exposed embryos (Fig. 3F, H) and still not detectable in embryos kept in normal seawater (Fig. 3E, G). Expression of *cyp1a* was also stronger in the skin and vasculature of B[a]P-exposed embryos (Fig. 3J) compared to the control group (Fig. 3I). *cyp1a* transcripts were also present in the heart and in the liver of embryos from both groups (Fig. 3L, M, O, P). No visible *cyp1a* expression was detected in the retinal layers of the control group (Fig. 3I, K) or the exposed group (Fig. 3J, N). However, some faint staining was seen in the lens in the control group, but this might be due to probe being trapped in the lens (Fig. 3K).

The specific expression of *ahr1a* in the eye was not clearly visible in the 3 dph whole mount larvae (Fig. 4A, B), but tissue sections revealed a persistent *ahr1a* expression in the ganglion cell and inner nuclear layers in larvae from both groups (Fig. 4C, D). At this stage, the

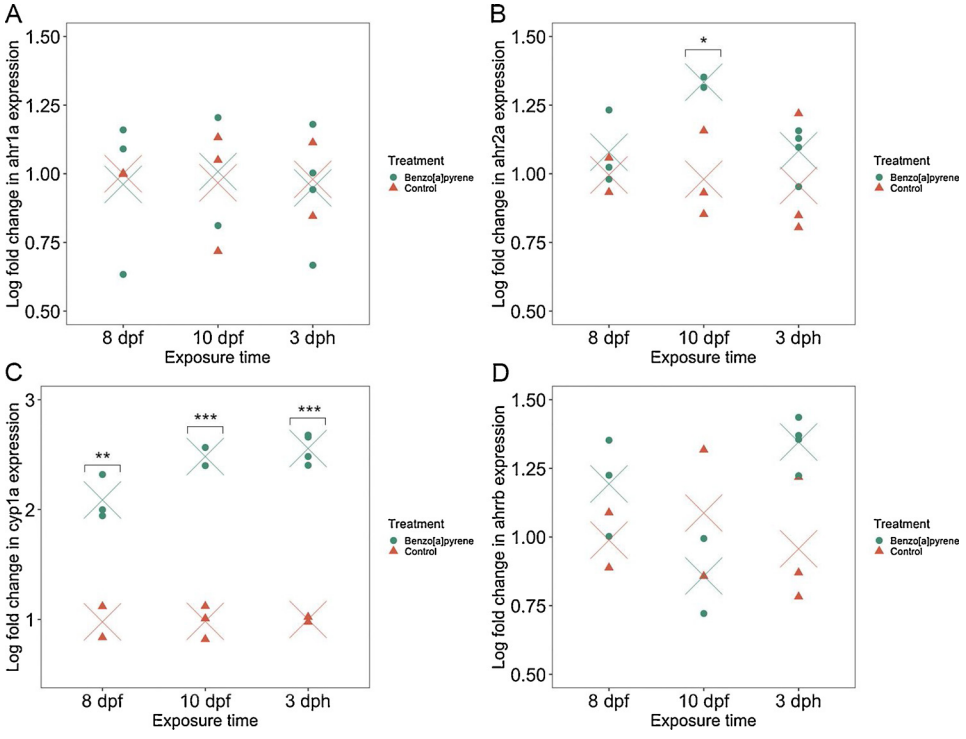

Fig. 1. Expression of *ahr1a, ahr2a, cyp1a* and *ahrrb* in B[a]P-exposed embryos and larvae. Atlantic cod eggs and larvae were exposed to B[a]P in a passive-dosing system using infused silicone rods. Expression of *ahr1a* (a) *ahr2a* (b) *cyp1a* (c) and *ahrrb* (d) was measured with qPCR at 8 days post fertilization (dpf), 10 dpf and 3 days post hatching (dph). Log fold change in gene expression was calculated in comparison with the control group (normal seawater). Pool of 10 embryos or larvae ($n = 4$) were collected from each beaker, but some samples were compromised during laboratory analysis. The data are presented as normalized values (points) and mean (cross). Statistical differences in log transformed transcript levels between control and B[a]P-exposed samples at the different sampling points were assessed by using a Welch *t*-test in R v1.2.1335 software. Level of statistical significance is indicated with *($p \leq 0.05$), **($p \leq 0.01$) or *** ($p \leq 0.001$).

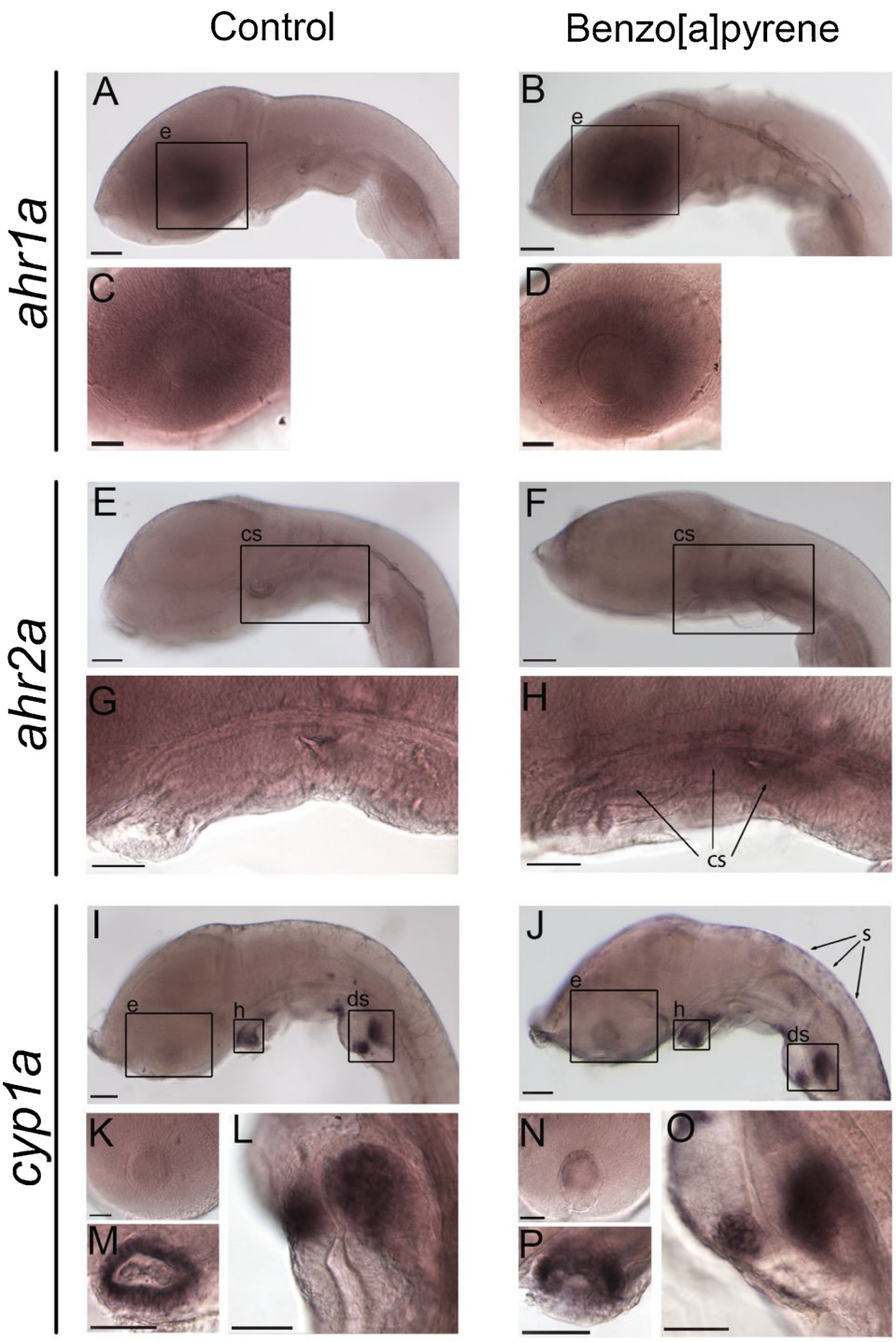

Fig. 2. Whole mount *in situ* hybridization of control and B[a]P-exposed Atlantic cod embryos at 8 dpf. Expression of *ahr1a*, *ahr2a* and *cyp1a* was assessed in both B[a]P-exposed and control samples. All pictures show dorsal view of either the whole embryo (A, B, E, F, I and J) or detailed areas where gene expression was visible. Pictures of the eye (C, D, K, N), cardiovascular system (G, H), digestive system (L, O), and heart (M, P) areas were imaged. Gene expression was visualized by specific DIG-labelled RNA probes. e; eye, cs; cardiovascular system, h; heart, ds; digestive system, s; skin. Scale bars: 100 μm in the whole embryo pictures and 500 nm in the detailed areas pictures.

expression of *ahr2a* was also intense in the cardiovascular system of B[a]P-exposed larvae (Fig. 4F) compared to the controls (Fig. 4E). In addition, expression of *ahr2a* was also detectable in the jaws, heart and fin nodes in larvae from both groups (Fig. 4G, H, J, K, M) and mainly in the liver area bordering towards the intestine of B[a]P-exposed individuals (Fig. 4L). In contrast to control larvae, there was a strong expression of *cyp1a* in the skin and vasculature of B[a]P-treated larvae, which made it difficult to capture the inner structures with conventional microscopy (Fig. 4N, O). However, *in situ* hybridization on tissue sections confirmed the presence of *cyp1a* in the heart and presumably the head kidney of both groups (Fig. 4Q, R, T, U) and in the liver and intestine of B[a]P-exposed samples (Fig. 4S). There was no expression of *ahr2a* or *cyp1a* in the liver from control larvae (Fig. 4I, P), but both *ahr2a* and *cyp1a* transcripts was observed in the liver of B[a]P-exposed larvae (Fig. 4L, S). Expression of those genes was also present in the heart of larvae from both groups, independent of the exposure regime (Fig. 4H, K).

3.4. Analyses of craniofacial and cardiac anomalies

No clearly visible malformations were observed in B[a]P-exposed 3 dph larvae, but differences in the length of jaw and ethmoid plate, edema area and FS between groups were measured for assessing putative deformities that can be produced after exposure to PAHs in early life stages (Table S2). Jaw lengths did not differ significantly between groups, and no consistent deviations in the length of the ethmoid plate

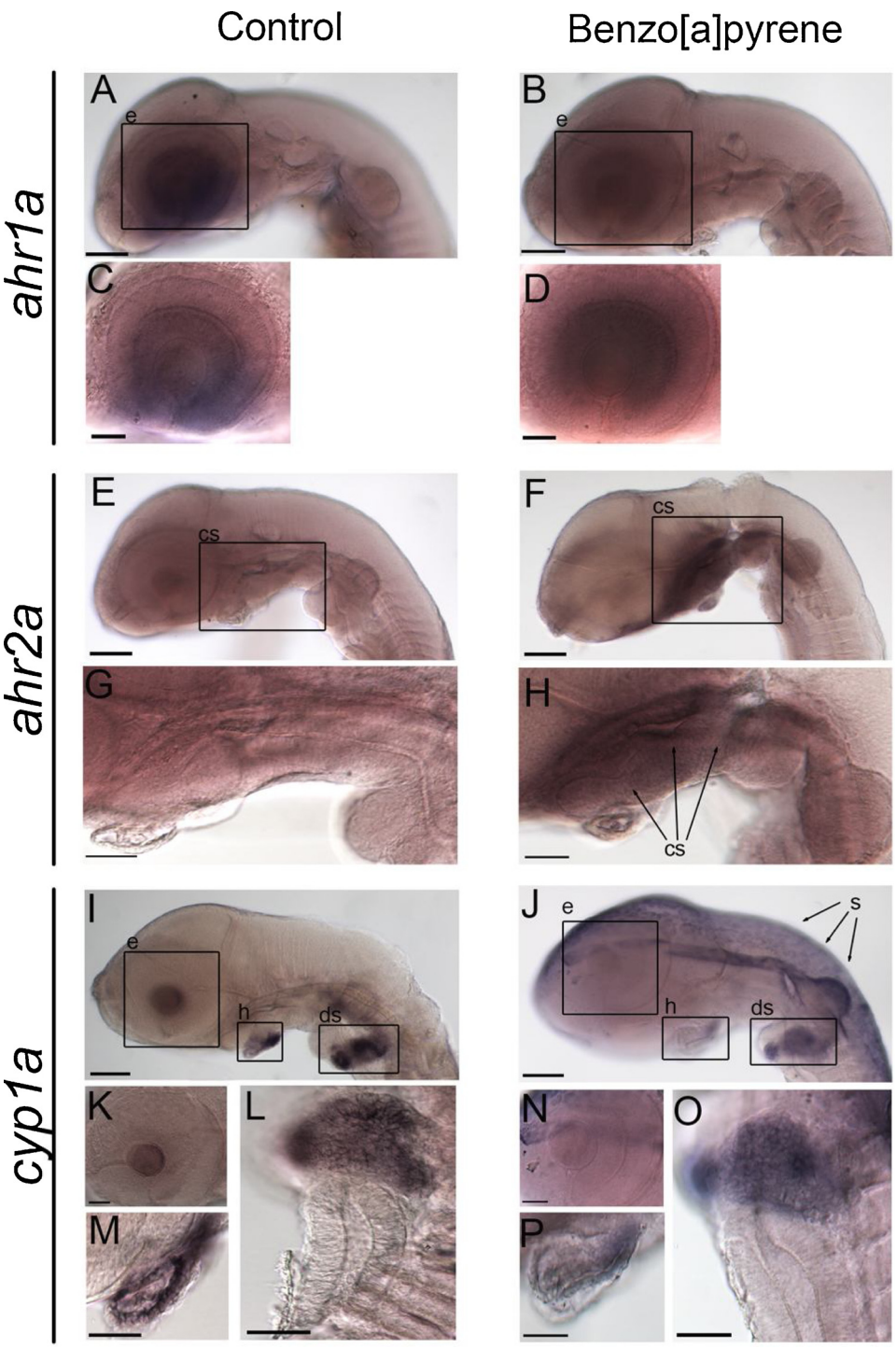

Fig. 3. Whole mount *in situ* hybridization of control and B[a]P-exposed Atlantic cod embryos at 10 dpf. Expression of *ahr1a*, *ahr2a* and *cyp1a* was assessed in both B[a]P-exposed and control samples. All pictures show dorsal view of either the whole embryo (A, B, E, F, I and J) or detailed areas where gene expression was visible. Pictures of the eye (C, D, K, N), cardiovascular system (G, H), digestive system (L, O), and heart region (M, P) were imaged. Gene expression was visualized by specific DIG-labelled RNA probes. e; eye, cs; cardiovascular system, h; heart, ds; digestive system, s; skin. Scale bars: 100 μm in the whole embryo pictures and 500 nm in the detailed areas pictures.

was revealed across the whole sample set (Table S2). Edema was not detected in 3 dph B[a]P-exposed larvae, nor any alterations in FS between control and B[a]P-exposed groups.

4. Discussion

In situ hybridization was used to study a possible subfunction partitioning of Ahr1a and Ahr2a in Atlantic cod by mapping the expression and localization of *ahr1a*, *ahr2a* and *cyp1a* during early development. Quantitative measurements showed an induction of the Ahr-target gene *cyp1a* at the different developmental stages assessed, confirming the activation of the Ahr-signaling pathway after B[a]P-exposure. An effect of B[a]P-exposure was also clearly visible in the skin of embryos and larvae where *cyp1a* was strongly expressed. Furthermore, the induction of *ahr2a* transcripts in the cardiovascular system of B[a]P-exposed embryos further supports an early effect of B[a]P on the Ahr-signaling pathway.

The purpose of the passive-dosing technique was to establish and maintain maximum aqueous B[a]P exposure. The measured concentrations of B[a]P in the exposure water had high variation but were reasonable in the context of solubility limits and anticipated deviations arising from experimental conditions. The published solubility of B[a]P in pure water is 1.52 μg/L at 25 °C (Schwarzenbach et al., 2003). Our measurements were somewhat higher than the published value, despite

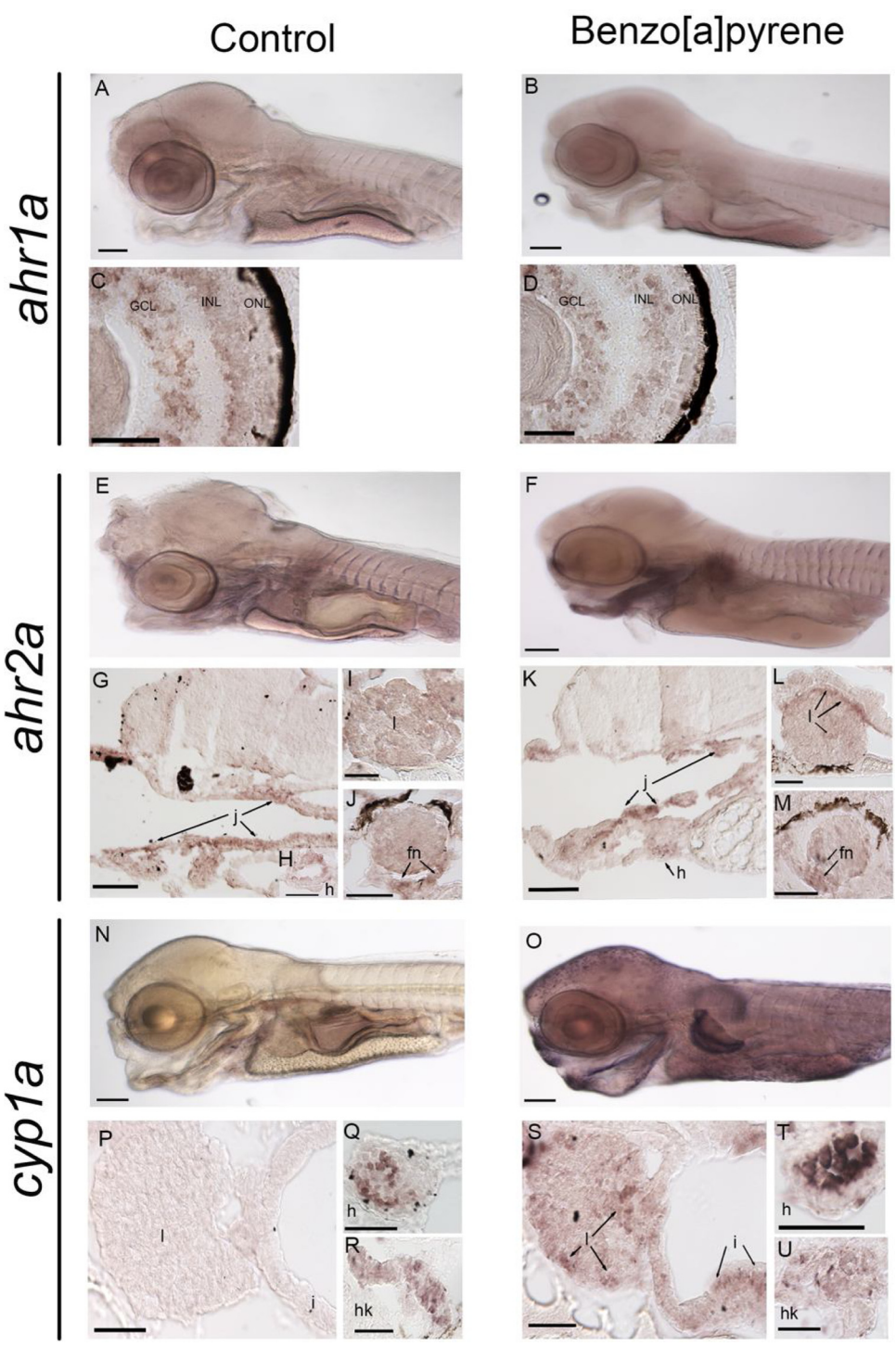

Fig. 4. *In situ* hybridization of whole mount and tissue sections prepared from control and B[a]P-exposed Atlantic cod larvae at 3 dph. Expression of *ahr1a*, *ahr2a* and *cyp1a* was assessed in both B[a]P-exposed and control samples. All pictures show dorsal view of either the whole larvae (A, B, E, F, N, O) or sectioned larvae. Pictures of the sectioned eye (C, D), jaws (G, K), heart (H, K,Q,T), liver (I, L, P, S), intestine (P, S), fin nodes (J, M), and presumably head kidney region (R, U) were imaged. Gene expression was visualized by specific DIG-labelled RNA probes. gcl; ganglion cell layer, inl; innear nuclear layer, onl; outer nuclear layer, j; jaws, h; heart, l; liver, fn; fin nodes, i; intestine, hk; head kidney. Scale bars: 100 μm in whole mount larvae and 500 nm in tissue sections except, 100 μm in G and K.

colder temperature and higher salinity, both of which should lower solubility. Binding of B[a]P to dissolved and particulate organic matter was the likely cause for the elevated and varying concentration measurements. The body burden analyses confirmed uptake of B[a]P into exposed fish embryos, while the actual body burdens were rather low. The uptake of B[a]P from aqueous media is limited by its very low solubility that is the combined result of a high hydrophobicity and high melting enthalpy (Kwon et al., 2016; Mayer and Reichenberg, 2006). However, the limited uptake is in line with previous passive-dosing exposure studies with *Daphnia magna* (Smith et al., 2010) and *Lumbriculus variegatus* (Agbo et al., 2013). Low body burdens can also be the results of biotransformation of B[a]P. At this developmental stage the liver bud is visible in Atlantic cod (Hall et al., 2004), and hepatic Cyp1a-mediated metabolism of B[a]P in fish has been demonstrated previously, including at early life stages during ontogenesis of the liver (Hornung et al., 2007; Kocan and Landolt, 1984; Stegeman et al., 1984; Stein et al., 1984; Varanasi et al., 1985). Low body burdens and efficient metabolism of B[a]P may also explain why the characeristic craniofacial and cardiac malformations often observed in early life stages of fish exposed to PAHs (Incardona, 2017) were not clearly visible in B[a]P-exposed cod larvae 3 dph.

Molecular mechanisms and physiological impacts of PAH-toxicity have been shown to differ among individual PAHs, and three possible modes of action have been described previously: Ahr-independent, Ahr-

dependent, and Cyp1a metabolism-dependent (Billiard et al., 2006; Clark et al., 2010; Incardona et al., 2005, 2006). B[a]P is a 5-ring PAH and well-known environmental pollutant with thoroughly characterized cytotoxic, genotoxic, mutagenic and carcinogenic properties (Juhasz and Naidu, 2000; Uno et al., 2001; Verma et al., 2012). B[a]P toxicity has previously been shown to affect the developing heart and cardiovascular system of zebrafish embryos (Huang et al., 2012; Incardona et al., 2011) by modulating the activity of Ahr2 and induce *cyp1a* expression in the heart in an Ahr-dependent mode of action (Incardona et al., 2011). Similarly, expression of *ahr2a* was mainly visible in the cardiovascular system of exposed cod embryos and larvae, and in the heart of 3 dph larvae, indicating cardiotoxicity responses to B[a]P-exposure at the different developmental stages assessed. Notably, the heart is the first organ to become functional in fish, and this process is finalized in Atlantic cod around the golden eye stage. Around 8 dpf (40-somite stage) the tubular heart is present, but looping, demarcation of the atrium and ventricle chambers, and formation of the two minor chambers (sinous venosus and the bulbous arteriosus) occurs later in development (Hall et al., 2004). The heart is fully formed at 10 dpf (golden stage) as a result of an increase in the myocardial mass, which is produced by cell differentiation or proliferation (de Pater et al., 2009). Even though expression of *ahr2a* in the heart of B[a]P-exposed embryos was not clearly visible when using whole mount *in situ* hybridization, the presence of *ahr2a* in the cardiovascular system indicates an expression of this gene also in the heart of cod embryos. Moreover, the slight quantitatively increase in *ahr2a* mRNA expression observed in 10 dpf B[a]P-exposed embryos may be linked to the increase in myocardial cells during embryonic development.

Strong induction of *cyp1a* transcripts was revealed with quantitative measurements, and abundant expression of this gene was localized to the skin and vasculature in B[a]P-exposed individuals. Induction of *cyp1a* after B[a]P exposure has been previously observed in Atlantic cod and several other teleost species (Aranguren-Abadía et al., 2020; Carlson et al., 2004; Incardona et al., 2011; Van Veld et al., 1997; Yadetie et al., 2018). Induced Cyp1a protein expression in the skin, vasculature and cardiovascular system was also reported in zebrafish embryos exposed to high doses of B[a]P (Incardona et al., 2011) and other PAHs (Shankar et al., 2019). Furthermore, other exposure studies using different Ahr agonists, such as 2,3,7,8-tetrachlorodibenzo-*p*-dioxin (TCDD) or β-naphthoflavone (BNF), have also reported increased *cyp1a* gene expression and Cyp1a protein synthesis in the skin, vasculature, and cardiovascular system of zebrafish embryos and larvae (Andreasen et al., 2002; Goodale et al., 2012; Sugden et al., 2017). The skin represents the first line of defence in a water exposure system, so expression of *cyp1a* in the epidermis of Atlantic cod embryos and larvae is not surprising.

The expression of both *ahr2a* and *cyp1a* was induced in the liver of B[a]P-exposed 3 dph cod larvae. Similar observations were made by Andreasen et al., 2002, which observed expression of these two genes in the cardiovascular system and in organs such as skin, heart, liver and head kidney of zebrafish larvae after TCDD exposure (Andreasen et al., 2002). Taken together, our results indicate a role of Ahr2a in mediating toxicity to B[a]P in early life stages of Atlantic cod, which apparently involves Ahr2a-mediated induction of *cyp1a* gene expression. Developmental toxicology studies using zebrafish embryos have also previously demonstrated that Ahr2 is the main subtype involved in mediating toxic responses by inducing *cyp1a* expression (Goodale et al., 2012; Incardona et al., 2011; Prasch et al., 2003; Tanguay et al., 1999). We have recently characterized molecular and functional properties of the Atlantic cod Ahr1a and Ahr2a receptors, and our results showed transcriptional activation of both Ahr1a and Ahr2a *in vitro* after exposure to different Ahr ligands, including B[a]P. However, the high abundancy of *ahr2a* transcripts in the liver suggested that Ahr2a is the main protein involved in mediating xenobiotic responses in juvenile Atlantic cod (Aranguren-Abadía et al., 2020). Notably, the presence of *ahr2a* and *cyp1a* transcripts in the heart, liver, and presumably the head kidney, at the different developmental stages independent of the exposure regimes, indicates also a physiological role of these genes during early development of Atlantic cod. It has been hypothesized that Ahr's original function was to regulate the development of neural systems and sensory structures (Emmons et al., 1999; Hahn et al., 2017). In vertebrates, it has been shown that Ahr regulates different signalling pathways and physiological systems, such as the cardiovascular, reproductive and immune system (Esser and Rannug, 2015; Larigot et al., 2018; Mulero-Navarro and Fernandez-Salguero, 2016; Nebert, 2017). The expression of *ahr2a* in the jaws and fin nodes in both 3 dph B[a]P-exposed and control larvae suggests a physiological role of *ahr2a* in ontogenesis of these organs. Several studies have also demonstrated that zebrafish Ahr2 has a role in the development of the neuronal and reproductive systems (Garcia et al., 2018; Goodale et al., 2012; Souder and Gorelick, 2019). It was recently demonstrated that Ahr2-null zebrafish adults had malformed cranial skeletal bones and severely damaged fins (Garcia et al., 2018). Another study also showed craniofacial malformations and irregularities in the development of fins in Ahr2 knock-out zebrafish embryos (Souder and Gorelick, 2019). Hence, a role of Ahr2a in mediating the development of Atlantic cod's jaws and fins is not unlikely. In addition, a role of CYP1A in metabolizing endogenous compounds has also recently been postulated (Lu et al., 2020) and may explain the expression of *cyp1a* in control embryos and larvae tissues.

Importantly, the eye was the only tissue were *ahr1a* transcripts were detected at all developmental stages assessed. Staining was strong in the ganglion cell layer already in 8 dpf embryos, and expression of *ahr1a* was also present in the eye inner cell layer of 3 dph larvae. In juvenile Atlantic cod, *ahr1a* expression was found in liver, brain and gill tissue, in addition to the eye (Aranguren-Abadía et al., 2020). A physiological role of the zebrafish *ahr1b* in embryonic development was postulated after high levels of *ahr1b* transcripts were detected in zebrafish embryos (Karchner et al., 2005). Recently, Karchner et al. have identified zfAhr1b protein in the inner plexiform and outer plexiform layers in the developing eye of zebrafish, and a down-regulation in the expression of genes involved in phototransduction in zfAhr1b knockdown embryos (Karchner et al., 2017). Different localization between cod *ahr1a* transcripts and zebrafish Ahr1b proteins in the eye layers may be explained by a translocation of Ahr1b to the plexiform layers subsequently to protein synthesis. Importantly, our results indicate that Atlantic cod's Ahr1a protein may be involved in embryonic development of the eye.

5. Conclusions

The spatio-temporal expression patterns of *ahr1a, ahr2a, and cyp1a* were mapped during early development of Atlantic cod. Different expression levels and localization of *ahr2a* and *cyp1a* transcripts were observed between control and B[a]P-exposed embryos and larvae at all developmental stages assessed. In B[a]P-exposed embryos and larvae the expression of *ahr2a* was mainly localized in the cardiovascular system, whereas *cyp1a* was mainly induced in the skin and vasculature. The presence of *ahr2a* and *cyp1a* in the liver of B[a]P-exposed larvae further supports a role of Ahr2a in mediating responses to xenobiotics in early life stages. Furthermore, the expression of *ahr1a* in the eye of both embryos and larvae, and the presence of *ahr2a* in the jaws and find nodes of larvae, also suggest roles of these proteins in ontogenesis during early development. Importantly, our data support that a subfunction partitioning of Ahr1a and Ahr2a has occurred in Atlantic cod.

Author contributions

LA-A, CED, ES, SM were involved in experimental design and sampling. LA-A performed RNA extraction and qPCR analyses, probe-design and synthesis, whole mount *in situ* hybridization analyses, whole mount and tissue section samples imaging, craniofacial and cardiac

measurements, and statistical analyses. CED analyzed water chemistry and body burden samples. ME contributed with whole mount *in situ* hybridization, and NG and VT performed *in situ* hybridization on tissue sections. ES contributed with the craniofacial and cardiac analyses, PM with expertise in passive-dosing techniques and TON and VT with *cyp1a* plasmid preparation. LA-A, CED, and OAK wrote the manuscript, with LA-A as the lead author. All authors contributed with interpretation of the results and revision of the manuscript.

Funding

This work was supported by Research Council of Norway (iCod 2.0: Integrative environmental genomics of Atlantic cod project (project no. 244564)), (EGGTOX: Unraveling the mechanistic effects of crude oil toxicity during early life stages of cold-water marine teleosts (project no. 267820)), (The effect of narrow banded LED light on development and growth performance (project no. 254894)), the Center for Digital Life Norway (dCod 1.0: decoding systems toxicology of Atlantic cod project, (project no. 248840) and by the Norwegian Research Center (NORCE).

Declaration of Competing Interest

The authors declare that they have no known competing financial interests or personal relationships that could have appeared to influence the work reported in this paper.

Acknowledgments

We thank the Institute of Marine Research (IMR) for providing farmed Atlantic cod and the facilities to perform the experiment. We also wish to thank Jon Vidar Helvik for letting L.A-A perform the *in situ* hybridization analyses at his laboratory and for helping with the design of the probes and imaging analyses, to Pål Olsvik for helping with the analyses of the qPCR data, to Knut Helge Jensen for helping with statistical analysis, to John Incardona for helping with the design of the experiment, to Mark E. Hahn for reading the manuscript, and to Anna Reboa, Lars Eirik Myklatun and Charlotte L. Nakken for technical assistance.

Appendix A. Supplementary data

Supplementary material related to this article can be found, in the online version, at doi:https://doi.org/10.1016/j.aquatox.2020.105558.

References

Agbo, S.O., Keinänen, M., Keski-Saari, S., Lemmetyinen, J., Akkanen, J., Leppänen, M.T., Mayer, P., Kukkonen, J.V.K., 2013. Changes in Lumbriculus variegatus metabolites under hypoxic exposure to benzo(a)pyrene, chlorpyrifos and pentachlorophenol: consequences on biotransformation. Chemosphere 93 (2), 302–310. https://doi.org/10.1016/j.chemosphere.2013.04.082.

Anderson, J.W., Neff, J.M., Cox, B.A., Tatem, H.E., Hightower, G.M., 1974. Characteristics of dispersions and water-soluble extracts of crude and refined oils and their toxicity to estuarine crustaceans and fish. Mar. Biol. 27 (1), 75–88. https://doi.org/10.1007/BF00394763.

Andreasen, E.A., Spitsbergen, J.M., Tanguay, R.L., Stegeman, J.J., Heideman, W., Peterson, R.E., 2002. Tissue-Specific Expression of AHR2, ARNT2, and CYP1A in Zebrafish Embryos and Larvae : Effects of Developmental Stage and 2,3,7,8-Tetrachlorodibenzo- p -dioxin Exposure. Toxicol. Sci. 68, 403–419.

Aranguren-Abadía, L., Lille-Langøy, R., Madsen, A.K., Karchner, S.I., Franks, D.G., Yadetie, F., Hahn, M.E., Goksøyr, A., Karlsen, O.A., 2020. Molecular and functional properties of the Atlantic Cod (*Gadus morhua*) aryl hydrocarbon receptors Ahr1a and Ahr2a. Environ. Sci. Technol. 54 (2), 1033–1044. https://doi.org/10.1021/acs.est.9b05312.

Barron, M.G., Heintz, R., Rice, S.D., 2004. Relative potency of PAHs and heterocycles as aryl hydrocarbon receptor agonists in fish. Mar. Environ. Res. 58 (2–5), 95–100. https://doi.org/10.1016/j.marenvres.2004.03.001.

Beyer, J., Sandvik, M., Hylland, K., Fjeld, E., Egaas, E., Aas, E., Skåre, J.U., Goksøyr, A., 1996. Contaminant accumulation and biomarker responses in flounder (Platichthys flesus L.) and Atlantic cod (Gadus morhua L.) exposed by caging to polluted sediments in Sørfjorden, Norway. Aquat. Toxicol. 36 (1–2), 75–98. https://doi.org/10.1016/S0166-445X(96)00798-9.

Billiard, S.M.S.M., Timme-Laragy, A.R., Wassenberg, D.M., Cockman, C., Di Giulio, R.T., 2006. The role of the aryl hydrocarbon receptor pathway in mediating synergistic developmental toxicity of polycyclic aromatic hydrocarbons to zebrafish. Toxicol. Sci. 92 (2), 526–536. https://doi.org/10.1093/toxsci/kfl011.

Carlson, E.A., Li, Y., Zelikoff, J.T., 2004. Benzo[a]pyrene-induced immunotoxicity in Japanese medaka (Oryzias latipes): relationship between lymphoid CYP1A activity and humoral immune suppression. Toxicol. Appl. Pharmacol. 201 (1), 40–52. https://doi.org/10.1016/j.taap.2004.04.018.

Carver, L.A., Bradfield, C.A., 1997. Ligand-dependent interaction of the aryl hydrocarbon receptor with a novel immunophilin homolog in vivo*. J. Biol. Chem. 272 (17), 11452–11456.

Chlebowski, A.C., Garcia, G.R., La Du, J.K., Bisson, W.H., Truong, L., Simonich, S.L.M., Tanguay, R.L., 2017. Mechanistic investigations into the developmental toxicity of nitrated and heterocyclic PAHs. Toxicol. Sci. 157 (1), 246–259. https://doi.org/10.1093/toxsci/kfx035.

Chomczynski, P., 1993. A reagent for the single-step simultaneous isolation of RNA, DNA and proteins from cell and tissue samples. Biotechniques 15 (3) 532-4,536-7.

Clark, B.W., Matson, C.W., Jung, D., Di Giulio, R.T., 2010. AHR2 mediates cardiac teratogenesis of polycyclic aromatic hydrocarbons and PCB-126 in Atlantic killifish (Fundulus heteroclitus). Aquat. Toxicol. 99 (2), 232–240. https://doi.org/10.1016/j.aquatox.2010.05.004.

Crawley, M.J., 2012. The R Book, second. Wiley.

Dale, K., Müller, M.B., Tairova, Z., Khan, E.A., Hatlen, K., Grung, M., Yadetie, F., Lille-Langøy, R., Blaser, N., Skaug, H.J., Lyche, J.L., Arukwe, A., Hylland, K., Karlsen, O.A., Goksøyr, A., 2019. Contaminant accumulation and biological responses in Atlantic cod (Gadus morhua) caged at a capped waste disposal site in Kollevåg, Western Norway. Mar. Environ. Res. 145, 39–51. https://doi.org/10.1016/j.marenvres.2019.02.003.

de Pater, E., Clijsters, L., Marques, S.R., Lin, Y.F., Garavito-Aguilar, Z.V., Yelon, D., Bakkers, J., 2009. Distinct phases of cardiomyocyte differentiation regulate growth of the zebrafish heart. Development 136 (10), 1633–1641. https://doi.org/10.1242/dev.030924.

Denison, M.S., Nagy, S.R., 2003. Activation of the Aryl hydrocarbon receptor by structurally diverse exogenous and endogenous chemicals. Annu. Rev. Pharmacol. Toxicol. 43 (1), 309–334. https://doi.org/10.1146/annurev.pharmtox.43.100901.135828.

Denison, M.S., Soshilov, A.A., He, G., Degroot, D.E., Zhao, B., 2011. Exactly the same but different : promiscuity and diversity in the molecular mechanisms of action of the aryl hydrocarbon (dioxin) receptor. Toxicol. Sci. 124 (1), 1–22. https://doi.org/10.1093/toxsci/kfr218.

Ebbesson, L.O.E., Nilsen, T.O., Helvik, J.V., Tronci, V., Stefansson, S.O., 2011. Corticotropin-releasing factor neurogenesis during midlife development in salmon: genetic, environmental and thyroid hormone regulation. J. Neuroendocrinol. 23 (8), 733–741. https://doi.org/10.1111/j.1365-2826.2011.02164.x.

Emmons, R.B., Duncan, D., Estes, P.A., Kiefel, P., Mosher, J.T., Sonnenfeld, M., Ward, M.P., Duncan, I., Crews, S.T., 1999. The spineless-aristapedia and tango bHLH-PAS proteins interact to control antennal and tarsal development in Drosophila. Development 126 (17), 3937–3945.

Esser, C., Rannug, A., 2015. The aryl hydrocarbon receptor in barrier organ physiology, immunology, and toxicology. Pharmacol. Rev. 67 (2), 259–279. https://doi.org/10.1124/pr.114.009001.

Garcia, G.R., Bugel, S.M., Truong, L., Spagnoli, S., Tanguay, R.L., 2018. AHR2 required for normal behavioral responses and proper development of the skeletal and reproductive systems in zebrafish. PLoS One 13 (3), 1–21. https://doi.org/10.1371/journal.pone.0193484.

Glasauer, S.M.K., Neuhauss, S.C.F., 2014. Whole-genome duplication in teleost fishes and its evolutionary consequences. Mol. Genet. Genom. 289 (6), 1045–1060. https://doi.org/10.1007/s00438-014-0889-2.

Goksøyr, A., Beyer, J., Husøy, A.M., Larsen, H.E., Westrheim, K., Wilhelmsen, S., Klungsøyr, J., 1994. Accumulation and effects of aromatic and chlorinated hydrocarbons in juvenile Atlantic cod (Gadus morhua) caged in a polluted fjord (Sørfjorden, Norway). Aquat. Toxicol. 29, 21–35. https://doi.org/10.1016/0166-445X(94)90045-0.

Goodale, B.C., la Du, J.K., Bisson, W.H., Janszen, D.B., Waters, K.M., Tanguay, R.L., 2012. AHR2 mutant reveals functional diversity of aryl hydrocarbon receptors in zebrafish. PLoS One 7 (1), 1–13. https://doi.org/10.1371/journal.pone.0029346.

Hahn, M.E., Karchner, S.I., Merson, R.R., 2017. Diversity as opportunity: insights from 600 million years of AHR evolution. Curr. Opin. Toxicol. 2, 58–71. https://doi.org/10.1016/j.cotox.2017.02.003.

Hall, T.E., Smith, P., Johnston, I.A., 2004. Stages of embryonic development in the Atlantic cod Gadus morhua. J. Morphol. 259 (3), 255–270. https://doi.org/10.1002/jmor.10222.

Hornung, M.W., Cook, P.M., Fitzsimmons, P.N., Kuehl, D.W., Nichols, J.W., 2007. Tissue distribution and metabolism of benzo[a]pyrene in embryonic and larval medaka (Oryzias latipes). Toxicol. Sci. 100 (2), 393–405. https://doi.org/10.1093/toxsci/kfm231.

Huang, L., Wang, C., Zhang, Y., Li, J., Zhong, Y., Zhou, Y., Chen, Y., Zuo, Z., 2012. Benzo [a]pyrene exposure influences the cardiac development and the expression of cardiovascular relative genes in zebrafish (Danio rerio) embryos. Chemosphere 87 (4), 369–375. https://doi.org/10.1016/j.chemosphere.2011.12.026.

Hylland, K., Tollefsen, K.E., Ruus, A., Jonsson, G., Sundt, R.C., Sanni, S., Røe Utvik, T.I., Johnsen, S., Nilssen, I., Pinturier, L., Balk, L., Barsiene, J., Marigòmez, I., Feist, S.W., Børseth, J.F., 2008. Water column monitoring near oil installations in the North Sea 2001-2004. Mar. Pollut. Bull. 56 (3), 414–429. https://doi.org/10.1016/j.marpolbul.2007.11.004.

Incardona, J.P., 2017. Molecular mechanisms of crude oil developmental toxicity in fish. Arch. Environ. Contam. Toxicol. 73 (1), 19–32. https://doi.org/10.1007/s00244-017-0381-1.

Incardona, J.P., Carls, M.G., Teraoka, H., Sloan, C.A., Collier, T.K., Scholz, N.L., 2005.

Aryl hydrocarbon receptor-independent toxicity of weathered crude oil during fish development. Environ. Health Perspect. 113 (12), 1755–1762. https://doi.org/10.1289/ehp.8230.
Incardona, J.P., Day, H.L., Collier, T.K., Scholz, N.L., 2006. Developmental toxicity of 4-ring polycyclic aromatic hydrocarbons in zebrafish is differentially dependent on AH receptor isoforms and hepatic cytochrome P4501A metabolism. Toxicol. Appl. Pharmacol. 217, 308–321. https://doi.org/10.1016/j.taap.2006.09.018.
Incardona, J.P., Linbo, T.L., Scholz, N.L., 2011. Cardiac toxicity of 5-ring polycyclic aromatic hydrocarbons is differentially dependent on the aryl hydrocarbon receptor 2 isoform during zebrafish development. Toxicol. Appl. Pharmacol. 257, 242–249. https://doi.org/10.1016/j.taap.2011.09.010.
Jönsson, M.E., Jenny, M.J., Woodin, B.R., Hahn, M.E., Stegeman, J.J., 2007. Role of AHR2 in the Expression of Novel Cytochrome P450 1 Family Genes, Cell Cycle Genes, and Morphological Defects in Developing Zebra Fish Exposed to 3,31',4,4',5-Pentachlorobiphenyl or 2,3,7,8-Tetrachlorodibenzo-p-dioxin. Toxicol. Sci. 100 (1), 180–193. https://doi.org/10.1093/toxsci/kfm207.
Jönsson, M.E., Franks, D.G., Woodin, B.R., Jenny, M.J., Garrick, R.A., Behrendt, L., Hahn, M.E., Stegeman, J.J., 2009. The tryptophan photoproduct 6-formylindolo[3,2-b] carbazole (FICZ) binds multiple AHRs and induces multiple CYP1 genes via AHR2 in zebrafish. Chem. Biol. Interact. 181 (3), 447–454. https://doi.org/10.1016/j.cbi.2009.07.003.
Juhasz, A.L., Naidu, R., 2000. Bioremediation of high molecular weight polycyclic aromatic hydrocarbons: a review of the microbial degradation of benzo[a]pyrene. International Biodeterioration and Biodegradation Vol. 45. Elsevier Science Ltd, pp. 57–88. https://doi.org/10.1016/S0964-8305(00)00052-4. Issues 1–2.
Karchner, S.I., Franks, D.G., Hahn, M.E., 2005. AHR1B, a new functional aryl hydrocarbon receptor in zebrafish: tandem arrangement of *ahr1b* and *ahr2* genes. Biochem. J. 392 (1), 153–161. https://doi.org/10.1042/BJ20050713.
Karchner, S., Jenny, M., Aluru, N., Franks, D., Laub, L., Linney, E., Williams, L., Teraoka, H., Hahn, M., 2017. Evidence for developmental versus toxicological roles for zebrafish AHR1b. Toxicol. Sci. (The Toxicological Supplement) 156 (S39). https://doi.org/10.1016/j.jhsa.2018.06.116. Abstract #1165.
Kazlauskas, A., Poellinger, L., Pongratz, I., 1999. Evidence that the co-chaperone p23 regulates ligand responsiveness of the dioxin (aryl hydrocarbon) receptor. J. Biol. Chem. 274 (19), 13519–13524. https://doi.org/10.1074/jbc.274.19.13519.
Knecht, A.L., Goodale, B.C., Truong, L., Simonich, M.T., Swanson, A.J., Matzke, M.M., Anderson, K.A., Waters, K.M., Tanguay, R.L., 2013. Comparative developmental toxicity of environmentally relevant oxygenated PAHs. Toxicol. Appl. Pharmacol. 271, 267–275. https://doi.org/10.1016/j.taap.2013.05.006.
Kocan, R.M., Landolt, M.L., 1984. Alterations in patterns of excretion and other metabolic functions in developing fish embryo exposed to benzo(a)pyrene. Helgolä¤nder Meeresunters. 37, 493–504.
Kwon, J.H., Lee, S.Y., Kang, H.J., Mayer, P., Escher, B.I., 2016. Including bioconcentration kinetics for the prioritization and interpretation of regulatory aquatic toxicity tests of highly hydrophobic chemicals. Environ. Sci. Technol. 50 (21), 12004–12011. https://doi.org/10.1021/acs.est.6b03942.
Larigot, L., Juricek, L., Dairou, J., Coumoul, X., 2018. AhR signaling pathways and regulatory functions. Biochim. Open 7, 1–9. https://doi.org/10.1016/j.biopen.2018.05.001.
Lu, J., Shang, X., Zhong, W., Xu, Y., Shi, R., Wang, X., 2020. New insights of CYP1A in endogenous metabolism: a focus on single nucleotide polymorphisms and diseases. Acta Pharm. Sin. B 10 (1), 91–104. https://doi.org/10.1016/j.apsb.2019.11.016.
Mayer, P., Reichenberg, F., 2006. Can highly hydrophobic organic substances cause aquatic baseline toxicity and can they contribute to mixture toxicity? Environ. Toxicol. Chem. 25 (10), 2639–2644. https://doi.org/10.1897/06-142R.1.
Mimura, J., Ema, M., Sogawa, K., Fujii-Kuriyama, Y., 1999. Identification of a novel mechanism of regulation of Ah (dioxin) receptor function. Genes Dev. 13 (1), 20–25. https://doi.org/10.1101/gad.13.1.20.
Mulero-Navarro, S., Fernandez-Salguero, P.M., 2016. New trends in aryl hydrocarbon receptor biology. Front. Cell Dev. Biol. 4 (May), 1–14. https://doi.org/10.3389/fcell.2016.00045.
Nebert, D.W., 2017. Aryl hydrocarbon receptor (AHR): "pioneer member" of the basic-helix/loop/helix per-Arnt-sim (bHLH/PAS) family of "sensors" of foreign and endogenous signals. Prog. Lipid Res. 67 (June), 38–57. https://doi.org/10.1016/j.plipres.2017.06.001.
Okey, A.B., 2007. An aryl hydrocarbon receptor odyssey to the shores of toxicology: the Deichmann Lecture, International Congress of Toxicology-XI. Toxicol. Sci. 98 (1), 5–38. https://doi.org/10.1093/toxsci/kfm096.
OSPAR, 2010. Background Document for Atlantic Cod Gadus morhua.
Perdew, G.H., 1988. Association of the ah receptor with the 90-kDa heat shock protein *. J. Biol. Chem. 263 (27), 13802–13805.
Pollenz, R.S., Sattler, C.A., Poland, A., 1993. The aryl hydrocarbon receptor and aryl hydrocarbon receptor nuclear translocator protein show distinct subcellular localizations in hepa 1 ci c7 cells by immunfluorescence microscopy. Mol. Pharmacol. 45, 428–438.
Prasch, A.L., Teraoka, H., Carney, S.A., Dong, W., Hiraga, T., Stegeman, J.J., Heideman, W., Peterson, R.E., 2003. Aryl hydrocarbon receptor 2 mediates 2,3,7,8-tetrachlorodibenzo-p-dioxin developmental toxicity in zebrafish. Toxicol. Sci. 76 (1), 138–150. https://doi.org/10.1093/toxsci/kfg202.
Sakurai, S., Shimizu, T., Ohto, U., 2017. The crystal structure of the AhRR–ARNT heterodimer reveals the structural basis of the repression of AhR-mediated transcription. J. Biol. Chem. 292 (43), 17609–17616. https://doi.org/10.1074/jbc.M117.812974.
Schwarzenbach, R., Gschwend, P., Imboden, D., 2003. Appendix table. Environmental Organic Chemistry, 2nd ed. John Wiley & Sons, Hoboken, New Jersey.
Shankar, P., Geier, M.C., Truong, L., McClure, R.S., Pande, P., Waters, K.M., Tanguay, R.L., 2019. Coupling genome-wide transcriptomics and developmental toxicity profiles in zebrafish to characterize polycyclic aromatic hydrocarbon (PAH) hazard. Int. J. Mol. Sci. 20 (10), 1–26. https://doi.org/10.3390/ijms20102570.
Smith, K.E.C., Dom, N., Blust, R., Mayer, P., 2010. Controlling and maintaining exposure of hydrophobic organic compounds in aquatic toxicity tests by passive dosing. Aquat. Toxicol. 98 (1), 15–24. https://doi.org/10.1016/j.aquatox.2010.01.007.
Sørensen, L., Meier, S., Mjøs, S.A., 2016. Application of gas chromatography/tandem mass spectrometry to determine a wide range of petrogenic alkylated polycyclic aromatic hydrocarbons in biotic samples. Rapid Commun. Mass Spectrom. 30 (18), 2052–2058. https://doi.org/10.1002/rcm.7688.
Sørensen, L., Hansen, B.H., Farkas, J., Donald, C.E., Robson, W.J., Tonkin, A., Meier, S., Rowland, S.J., 2019. Accumulation and toxicity of monoaromatic petroleum hydrocarbons in early life stages of cod and haddock. Environ. Pollut. 251, 212–220. https://doi.org/10.1016/j.envpol.2019.04.126.
Sørhus, E., Edvardsen, R.B., Karlsen, Ø., Nordtug, T., van der Meeren, T., Thorsen, A., Harman, C., Jentoft, S., Meier, S., 2015. Unexpected interaction with dispersed crude oil droplets drives severe toxicity in Atlantic Haddock Embryos. PLoS One 10 (4), e0124376. https://doi.org/10.1371/journal.pone.0124376.
Sørhus, E., Incardona, J.P., Karlsen, Ø., Linbo, T., Sørensen, L., Nordtug, T., Van Der Meeren, T., Thorsen, A., Thorbjørnsen, M., Jentoft, S., Edvardsen, R.B., Meier, S., 2016. Crude oil exposures reveal roles for intracellular calcium cycling in haddock craniofacial and cardiac development. Sci. Rep. 6 (31058), 1–21. https://doi.org/10.1038/srep31058.
Soshilov, A., Denison, M.S., 2008. Role of the Per/Arnt/Sim domains in ligand-dependent transformation of the aryl hydrocarbon receptor. J. Biol. Chem. 283 (47), 32995–33005. https://doi.org/10.1074/jbc.M802414200.
Souder, J.P., Gorelick, D.A., 2019. ahr2, but not ahr1a or ahr1b, is required for Craniofacial and Fin Development and TCDD- dependent Cardiotoxicity in Zebrafish. Toxicol. Sci. 170 (1), 25–44. https://doi.org/10.1093/toxsci/kfz075.
Stegeman, J.J., Woodin, B.R., Binder, R.L., 1984. Patterns of benzo[a]pyrene metabolism by varied species, organs, and developmental stages of fish. Use of Small Fish Species in Carcinogenecity Testing. pp. 371–378.
Stein, J.E., Hom, T., Casillas, E., Friedman, A., Varanasi, U., 1984. Simultaneous exposure of English sole (Parophrys vetulus) to sediment-associated xenobiotics: part 1-Uptake and Disposition of14C-Polychlorinated Biphenyls and 3H-Benzo[a]Pyrene. Mar. Environ. Res. 13, 97–119. https://doi.org/10.1016/0141-1136(87)90032-8.
Sugden, W.W., Leonardo-Mendonça, R.C., Acuña-Castroviejo, D., Siekmann, A.F., 2017. Genetic dissection of endothelial transcriptional activity of zebrafish aryl hydrocarbon receptors (AHRs). PLoS One 12 (8), 1–22. https://doi.org/10.1371/journal.pone.0183433.
Sundt, R.C., Ruus, A., Jonsson, H., Skarphédinsdóttir, H., Meier, S., Grung, M., Beyer, J., Pampanin, D.M., 2012. Biomarker responses in Atlantic cod (Gadus morhua) exposed to produced water from a North Sea oil field: laboratory and field assessments. Mar. Pollut. Bull. 64 (1), 144–152. https://doi.org/10.1016/j.marpolbul.2011.10.005.
Swanson, H.I., 2002. DNA binding and protein interactions of the AHR/ARNT heterodimer that facilitate gene activation. Chem. Biol. Interact. 141 (1–2), 63–76. https://doi.org/10.1016/S0009-2797(02)00066-2.
Tanguay, R.L., Abnet, C.C., Heideman, W., Peterson, R.E., 1999. Cloning and characterization of the zebrafish (Danio rerio) aryl hydrocarbon receptor. Biochimica Et 1444 (1), 35–48 https://doi.org/S0167-4781(98)00252-8 [pii].
Thisse, C., Thisse, B., 2008. High-resolution in situ hybridization to whole-mount zebrafish embryos. Nat. Protoc. 3, 59–69.
Uno, S., Dalton, T.P., Shertzer, H.G., Genter, M.B., Warshawsky, D., Talaska, G., Nebert, D.W., 2001. Benzo[a]pyrene-induced toxicity: paradoxical protection in Cyp1a1(-/-) knockout mice having increased hepatic BaP-DNA adduct levels. Biochem. Biophys. Res. Commun. 289 (5), 1049–1056. https://doi.org/10.1006/bbrc.2001.6110.
Valen, R., Edvardsen, R.B., Søviknes, A.M., Drivenes, Ø., Helvik, J.V., 2014. Molecular evidence that only two opsin subfamilies, the blue light- (SWS2) and green light-sensitive (RH2), drive color vision in Atlantic Cod (Gadus morhua). PLoS One 9 (12), 1–24. https://doi.org/10.1371/journal.pone.0115436.
Van Veld, P.A., Vogelbein, W.K., Cochran, M.K., Goksøyr, A., Stegeman, J.J., 1997. Route-specific cellular expression of cytochrome P4501A (CYP1A) in fish (Fundulus heteroclitus) following exposure to aqueous and dietary benzo[a]pyrene. Toxicol. Appl. Pharmacol. 142 (2), 348–359. https://doi.org/10.1006/taap.1996.8037.
Vandesompele, J., De Preter, K., Pattyn, F., Poppe, B., Van Roy, N., De Paepe, A., Speleman, F., 2002. Accurate normalization of real-time quantitative RT-PCR data by geometric averaging of multiple internal control genes. Rock Mech. Rock Eng. 3 (7), 1–12. https://doi.org/10.1007/s00603-018-1496-z.
Varanasi, U., Relchert, W.L., Stein, J.E., Brown, D.W., Sanborn, H.R., 1985. Bioavailability and biotransformation of aromatic hydrocarbons in benthic organisms exposed to sediment from an urban estuary. Environ. Sci. Technol. 19 (9), 836–841. https://doi.org/10.1021/es00139a012.
Verma, N., Pink, M., Rettenmeier, A.W., Schmitz-Spanke, S., 2012. Review on proteomic analyses of benzo[a]pyrene toxicity. PROTEOMICS 12 (11), 1731–1755. https://doi.org/10.1002/pmic.201100466.
Walker, M.K., Spitsbergen, J.M., Olson, J.R., Peterson, R.E., 1991. 2,3,7,8-Tetrachlorodibenzo-p-dioxin (TCDD) toxicity during early life stage development of lake trout (Salvelinus namaycush). Can. J. Fish. Aquat. Sci. 48, 875–883.
Whitlock, J.P.J., 1999. Induction of cytochrome P4501a1. Annu. Rev. Pharmacol. Toxicol. 39 (1), 103–125. https://doi.org/10.1146/annurev.pharmtox.39.1.103.
Yadetie, F., Zhang, X., Hanna, E.M., Aranguren-Abadía, L., Eide, M., Blaser, N., Brun, M., Jonassen, I., Goksøyr, A., Karlsen, O.A., 2018. RNA-Seq analysis of transcriptome responses in Atlantic cod (Gadus morhua) precision-cut liver slices exposed to benzo[a]pyrene and 17A-ethynylestradiol. Aquat. Toxicol. 201, 174–186. https://doi.org/10.1016/j.aquatox.2018.06.003.
Zanette, J., Jenny, M.J., Goldstone, J.V., Woodin, B.R., Watka, L.A., Bainy, A.C.D., Stegeman, J.J., 2009. New cytochrome P450 1B1, 1C2 and 1D1 genes in the killifish Fundulus heteroclitus: basal expression and response of five killifish CYP1s to the AHR agonist PCB126. Aquat. Toxicol. 93 (4), 234–243. https://doi.org/10.1016/j.aquatox.2009.05.008.